MARTIN MARIETTA ENERGY SYSTEMS LIBRARIES

3 4456 0360617 7

ORNL-1415
Progress

PHYSICS DIVISION

QUARTERLY PROGRESS REPORT

FOR PERIOD ENDING SEPTEMBER 20, 1952

CENTRAL RESEARCH LIBRARY
DOCUMENT COLLECTION

LIBRARY LOAN COPY

DO NOT TRANSFER TO ANOTHER PERSON

If you wish someone else to see this document, send in name with document and the library will arrange a loan.

OAK RIDGE NATIONAL LABORATORY
OPERATED BY
CARBIDE AND CARBON CHEMICALS COMPANY
A DIVISION OF UNION CARBIDE AND CARBON CORPORATION

UCC

POST OFFICE BOX P
OAK RIDGE, TENNESSEE

ORNL-1415

This document consists of 32 pages.

Copy 5 of 332 copies. Series A.

Contract No. W-7405-eng-26

PHYSICS DIVISION

QUARTERLY PROGRESS REPORT

for Period Ending September 20, 1952

A. H. Snell, Director
E. O. Wollan, Associate Director

DATE ISSUED

OAK RIDGE NATIONAL LABORATORY
operated by
CARBIDE AND CARBON CHEMICALS COMPANY
A Division of Union Carbide and Carbon Corporation
Post Office Box P
Oak Ridge, Tennessee

MARTIN MARIETTA ENERGY SYSTEMS LIBRARIES

3 4456 0360617 7

INTERNAL DISTRIBUTION

1. G. T. Felbeck (C&CCC)
2. Biology Library
3. Health Physics Library
4. Metallurgy Library
5-6. Central Research Library
7. Reactor Experimental Engineering Library
8-13. Central Files
14. C. E. Center
15. C. E. Larson
16. W. B. Humes (K-25)
17. L. B. Emlet (Y-12)
18. A. M. Weinberg
19. E. H. Taylor
20. E. D. Shipley
21. E. J. Murphy
22. F. C. VonderLage
23. A. H. Snell
24. J. A. Swartout
25. A. Hollaender
26. K. Z. Morgan
27. F. L. Steahly
28. M. T. Kelley
29. E. M. King
30. E. O. Wollan
31. D. W. Cardwell
32. A. S. Householder
33. L. D. Roberts
34. R. B. Briggs
35. R. N. Lyon
36. W. C. Koehler
37. W. K. Ergen
38. E. P. Blizard
39. M. E. Rose
40. G. E. Boyd
41. Lewis Nelson
42. R. W. Stoughton
43. C. E. Winters
44. W. H. Jordan
45. E. C. Campbell
46. D. S. Billington
47. M. A. Bredig
48. R. S. Livingston
49. C. P. Keim
50. J. L. Meem
51. C. E. Clifford
52. G. H. Clewett
53. C. D. Susano
54. C. J. Borkowski
55. M. J. Skinner
56. L. A. Rayburn
57. S. Bernstein
58. P. M. Reyling
59. D. D. Cowen
60. W. M. Good
61. G. C. Williams
62. E. P. Wigner (consultant)
63. H. A. Bethe (consultant)
64. K. Lark-Horovitz (consultant)
65. Eugene Guth (consultant)
66. J. G. Daunt (consultant)

EXTERNAL DISTRIBUTION

67. L. C. Biedenharn, Sloans Physics Laboratory
68. R. F. Bacher, California Institute of Technology
69-70. Ohio State University, Attn: Professor of Naval Science
71. John Dunning, Columbia University
72. Phillips Petroleum Co., Attn: Librarian
73. R. L. Heath, American Cyanamid Co.
74. S. DeBenedetti, Carnegie Institute of Technology
75. Massachusetts Institute of Technology, Department of Electrical Engineering
76. A. von Hippel, Laboratory for Insulation Research, MIT
77. M. Goodrich, Louisiana State University
78-332. Given distribution as shown in TID 4500 under Physics Category

Physics Division quarterly progress reports previously issued in this series are as follows:

ORNL-325 Supplement	December, January, and February, 1948-1949
ORNL-366	Period Ending June 15, 1949
ORNL-481	Period Ending September 25, 1949
ORNL-577	Period Ending December 15, 1949
ORNL-694	Period Ending March 15, 1950
ORNL-782	Period Ending June 15, 1950
ORNL-865	Period Ending September 20, 1950
ORNL-940	Period Ending December 20, 1950
ORNL-1005	Period Ending March 20, 1951
ORNL-1092	Period Ending June 20, 1951
ORNL-1164	Period Ending September 20, 1951
ORNL-1278	Period Ending December 20, 1951
ORNL-1289	Period Ending March 20, 1952
ORNL-1365	Period Ending June 20, 1952

CONTENTS

	Page
SUMMARY	1
1. HIGH-VOLTAGE PHYSICS	2
Angular Distribution of Neutrons Scattered from Nitrogen	2
The $Al^{27}(p,n)Si^{27}$ Threshold	3
The Reactions $H^3(p,n)He^3$ and $H^3(p,\gamma)He^4$	3
Reactions with the Cockcroft-Walton He^3 Beam	4
Lithium–6	4
Helium–3	5
Tritium	6
2. RADIOACTIVITY AND NUCLEAR ISOMERISM	8
Gamma-Ray Absorption and Scattering	8
Ratio of Peak to Total for a Thallium-activated Sodium Iodide Crystal	10
Gamma-Gamma Angular Correlations in Ta^{181} and Hf^{177}	12
3. NEUTRON DIFFRACTION	14
Paramagnetic Scattering of Neutrons by Trivalent Ions of Neodymium and Erbium	14
4. NEUTRON CROSS SECTIONS	15
Total Cross-Section Measurements with Time-of-Flight Spectrometer	15
Pile-Oscillator Measurements of Stable-Isotope Cross Sections	15
5. THEORETICAL PHYSICS	17
Auger Effect	17
Quantum Electrodynamics	18
Nuclear Three-Body Problem	19
Scattering of Slow Neutrons by Atoms with Nonzero Orbital Moments	19

PUBLICATIONS

The following papers by members of the Physics Division appeared in open publications during the last quarter:

E. D. Klema and R. H. Ritchie, "Thermal Neutron Flux Measurements in Graphite Using Gold and Indium Foils," *Phys. Rev.* **87**, 167 (1952).

S. Bernstein, L. B. Borst, C. P. Stanford, T. E. Stephenson, and J. B. Dial, "Slow Neutron Crystal Spectrometry: The Total Cross Sections of Co, Er, Hf, Ni^{58}, Ni^{60}, Ho, and Fission Sm," *Phys. Rev.* **87**, 487 (1952).

E. D. Klema and F. K. McGowan, "Gamma-Gamma Angular Correlation in Cd^{114}," *Phys. Rev.* **87**, 524 (1952).

F. K. McGowan, "Lifetime of an Excited State of Hf^{176}," *Phys. Rev.* **87**, 542 (1952).

J. Schenck, "Neutron-Detecting Phosphors," *Nucleonics* **10**, 54 (August 1952).

ANNOUNCEMENTS

The following personnel have been added to the staff of the Physics Division during this quarter: P. H. Stelson (high-voltage group); J. J. Lynn, R. A. Francis, Jr., and J. F. Ellis (ANP critical experiments).

Terminations for this period were as follows: E. V. Haake (ANP critical experiments); S. Tamor and L. C. Biedenharn (theoretical group); L. S. Abbot (shielding program); L. A. Rayburn and K. L. Robertson (neutron-diffraction studies).

PHYSICS DIVISION QUARTERLY PROGRESS REPORT

SUMMARY

High-Voltage Physics. The 2-Mev Van de Graaff was moved into the new, permanent High-Voltage Building during this period.

The elastic scattering of neutrons from nitrogen nuclei has been investigated from 0.8 to 2.4 Mev by use of the method of pulse-height analysis of recoil nitrogen nuclei. The distributions for nonresonance energies indicate pronounced forward scattering of neutrons.

The angular distribution of neutrons from the $H^3(p,n)He^3$ reaction has been remeasured as a function of energy. The target was tritium gas contained in a cell. The relative yield of gamma rays from the $H^3(p,\gamma)He^4$ reaction has been determined from 1 to 5.22 Mev by use of the same target.

The threshold of the $Al^{27}(p,n)Si^{27}$ reaction was found to be 5.819 ± 0.010 Mev.

Acceleration of pure He^3 in the Cockcroft-Walton machine has made possible a study of the reactions of He^3 with H^3, He^3, and Li^6. The energy spectra of charged particles associated with nine resulting reactions have been studied.

Radioactivity and Nuclear Isomerism. Results of measurements of gamma-ray absorption coefficients in sodium iodide are reported. Coherent-scattering cross sections were also measured and were found not to be in good agreement with theoretical expectations.

Further work is reported on the angular correlation of the gamma rays emitted during the decay of Hf^{181} and the dependence of the correlation on the chemical state of the source. The observed anisotropy is not readily accounted for.

Neutron Diffraction. The paramagnetic scattering of neutrons from the trivalent ions of neodymium and erbium has been measured. These ions are of special interest because of the large orbital contribution to the magnetic scattering for which the scattering theory has not yet been developed.

Neutron Cross Sections. The total cross sections of copper and thorium were measured with the time-of-flight spectrometer. Resonances for copper appear at 720 and 2200 ev, and six resonances for thorium were observed between 23 and 870 ev.

A new measurement with the pile oscillator of the capture cross section of vanadium gives $\sigma_c = 23 \pm 1$ barns. A measurement has also been made on a 2.5-curie source of Ac^{227}, which gives $\sigma_c = 500 \pm 35$ barns.

Theoretical Physics. Plans are discussed for calculations for the Auger process. These calculations are closely related to and can be advanced by the work being performed on the *L*-shell conversion problems.

It is pointed out in connection with the subject of quantum electrodynamics, which has been discussed in previous reports, that a number of new experiments might give valuable information for guiding the work in formulating the positron theory. One such experiment involves a study of the positron-induced deviation from the coulomb scattering of low-energy protons from light nuclei.

The nuclear three-body problem has been studied with the objective of putting the problem in a good form for computation with the digital computer that is scheduled for delivery to the Laboratory within the year.

A calculation of the effect of nonzero orbital moments on the magnetic scattering of neutrons has been made for the region of small $(\sin \theta)/\lambda$.

1. HIGH-VOLTAGE PHYSICS

ANGULAR DISTRIBUTION OF NEUTRONS SCATTERED FROM NITROGEN

J. L. Fowler C. H. Johnson
J. R. Risser[1]

The method of studying elastic scattering of neutrons by performing pulse-height analysis of nitrogen nuclei recoils in a counter gas[2] has been utilized on the 5-Mev Van de Graaff machine. The active volume of the proportional counter used is a cylinder 12.7 cm long and 7.62 cm in diameter. Field tubes[3] included in the counter design eliminate end effects that result from nonuniform electric fields. The counter wire is separated from the field-tube voltage by grounded shield tubes. The details of the counter design and fabrication were handled by R. E. Zedler of the Instrument Department.

A test with the 630-kev proton peak from the $N^{14}(n,p)C^{14}$ reaction produced by thermal neutrons indicated an energy resolution of the counting system of about 6% (full width at half maximum of the pulse-height distribution). Figure 1.1 shows the pulse-height distributions of the nitrogen recoils from monoenergetic neutrons produced by the $H^3(p,n)He^3$ reaction. Tritium contained in a gas cell was bombarded with analyzed protons from the 5-Mev Van de Graaff. The neutron energy spread caused by thickness of target and straggling of protons in the gas-cell window was of the order of ±20 kev. The energies chosen are those between the resonances in the total cross section reported in the literature.[4,5,6] These distributions have been corrected for an experimentally determined nonlinear dependence of maximum recoil pulse height on neutron energy. The background near zero pulse height has been subtracted

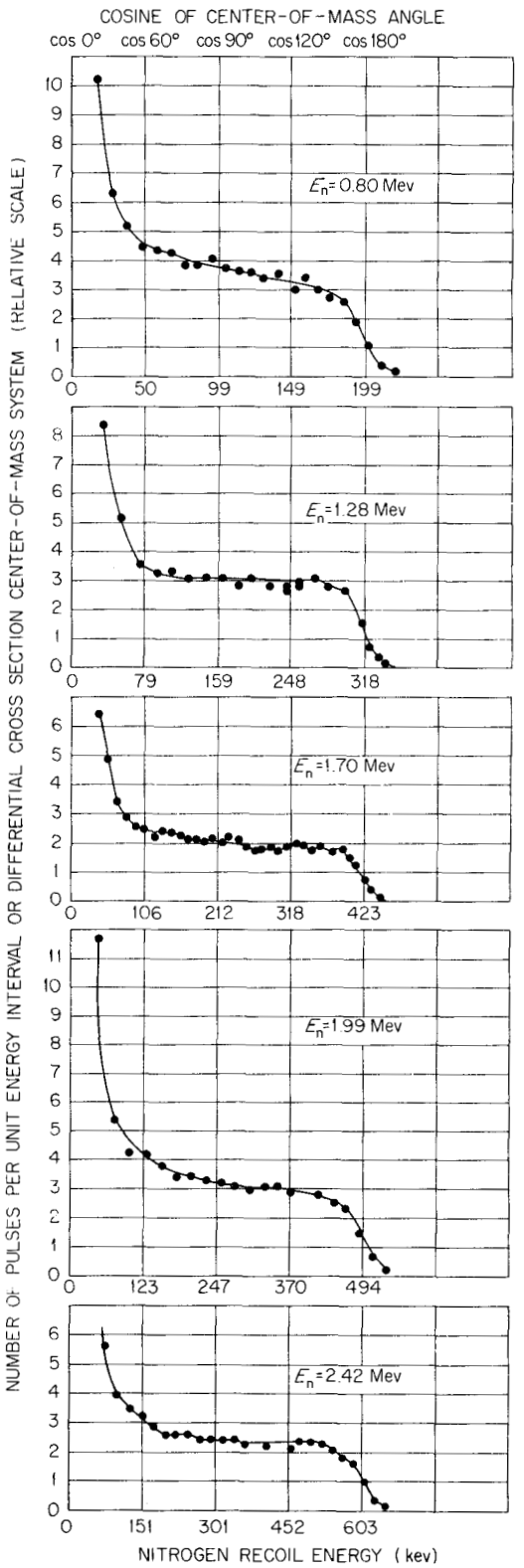

Fig. 1.1. Nitrogen Recoil Energy.

---

[1] Summer research participant.

[2] B. B. Rossi and H. H. Staub, *Ionization Chambers and Counters; Experimental Techniques*, p. 135, McGraw-Hill, New York, 1949.

[3] A. L. Cockroft and S. C. Curran, *Rev. Sci. Instruments* **22**, 37 (1951).

[4] C. H. Johnson, B. Petree, and R. K. Adair, *Phys. Rev.* **84**, 775 (1951).

[5] J. J. Hinchley, P. H. Stelson, and W. M. Preston, *Phys. Rev.* **86**, 483 (1952).

[6] C. H. Johnson, H. B. Willard, J. K. Bair, and J. D. Kington, *Phys. Quar. Prog. Rep. June 20, 1952*, ORNL-1365, p. 1.

from the distribution. This background was determined by substituting helium for tritium in the gas cell and was found to be completely negligible for the upper three-fourths of the distribution. The distribution at 0.8 Mev has been checked a number of times under a variety of experimental conditions:

1. The nitrogen pressure in the counter was changed by a factor of 3.
2. The counter voltage and consequently the gas multiplication was varied over a considerable range.
3. The tritium neutron source was altered; nickel was substituted for aluminum as the tritium cell window, and the experiment was performed with a zirconium tritide target.

With the exception of fluctuations near zero pulse height the distributions obtained were essentially the same. The number of nitrogen recoils per incident neutron can be predicted from the geometry and the nitrogen pressure by the use of known values of the total cross section.[4,5,6] The number of neutrons was determined with a long counter calibrated against a polonium-beryllium source. The comparison between the prediction and the number of counts in actual distributions extrapolated to zero energy indicated agreement within the accuracy of the neutron measurements.

The cosine of the center-of-mass angle of scattering of the neutron is plotted in Fig. 1.1 on the same horizontal scale with the recoil energy. The ordinate is thus proportional to the differential scattering cross section in the center-of-mass system.[2] The rise in the cross section at low angles, which is being investigated further, is believed to be real and to be due to shadow scattering.

Several distributions taken in going over the 1.595-Mev resonance[5] show a marked change in the differential cross section associated with the peak of the resonance.[7] Forward scattering of the neutrons becomes more pronounced at the resonance.

THE $Al^{27}(p,n)Si^{27}$ THRESHOLD

J. D. Kington J. K. Bair
H. B. Willard

The $Al^{27}(p,n)Si^{27}$ threshold has been determined as $E_{th} = 5.819 \pm 0.010$ Mev by using a Bonner-type counter as a detector.[8] The resulting Q value of −5.61 Mev gives 0.00519 atomic mass unit for the $Si^{27} - Al^{27}$ mass difference and 3.81 Mev for the maximum disintegration energy of Si^{27}.

THE REACTIONS $H^3(p,n)He^3$ AND $H^3(p,\gamma)He^4$

H. B. Willard J. K. Bair
J. D. Kington

The measurement of the angular distributions of neutrons from the proton bombardment of tritium[9] has been repeated by using a gas target as a source. Results show a more pronounced minimum in the center-of-mass system at 80 deg than was found previously with the tritium-zirconium target. It is assumed that the discrepancy is due to the rather large correction that had to be applied to the old data for absorption in the backing material and for in-scattering.

A relative yield curve of the 20-Mev gamma rays from the $H^3(p,\gamma)He^4$ reaction[10] has been obtained from 1 to 5.22 Mev as shown in Fig. 1.2.

(7) E. Baldinger, P. Huber, R. Ricamo, and W. Zünti, *Helv. Phys. Acta* 23, 503 (1950).

(8) H. B. Willard, J. K. Bair, T. M. Hahn, and J. D. Kington, *Phys. Quar. Prog. Rep. Sept. 20, 1951*, ORNL-1164, p. 25

(9) H. B. Willard, J. K. Bair, and J. D. Kington, *Phys. Quar. Prog. Rep. Dec. 20, 1951* ORNL-1278, p. 2.

(10) J. K. Bair, H. B. Willard, and J. D. Kington, *Phys. Quar. Prog. Rep. March 20, 1952*, ORNL-1289, p. 7.

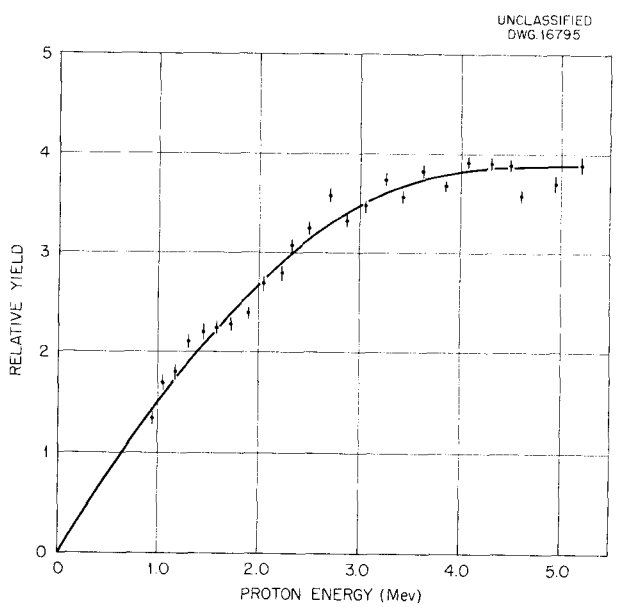

Fig. 1.2. $H^3(p,\gamma)He^4$ 90-deg Yield Curve.

REACTIONS WITH THE COCKCROFT-WALTON He^3 BEAM

W. M. Good W. E. Kunz
C. D. Moak

The He^{3+} output of the 400-kv Cockcroft-Walton accelerator has recently been increased from 5 to 200 μa by employing pure He^3 as feed gas to the ion source rather than a 5% He^3, 95% He^4 mixture. A He^{3++} current of 2 μa is now available and is being used to extend several cross-section measurements to the energy region of 800 kev. The increased current output has made feasible the re-examination, with improved energy resolution, of several reactions. By reducing the solid angle subtended by the counting equipment, the energy spread with angle resulting from center-of-mass motion has been reduced to less than 1% at any energy measured. The new spectrometer arrangement is shown in Fig. 1.3. A sodium iodide crystal, 2 mm thick, is mounted in the target vacuum and is covered with 700 μg of aluminum to stop He^3 particles scattered from the beam. The crystal is optically coupled to a 5819 photomultiplier by a Lucite button mounted in an "O"-ring vacuum seal. With this arrangement the reactions of He^3 on Li^6, He^3, and H^3 have been re-examined. In each case, only charged particles are observed; the spectra of these particles are discussed in the following sections.

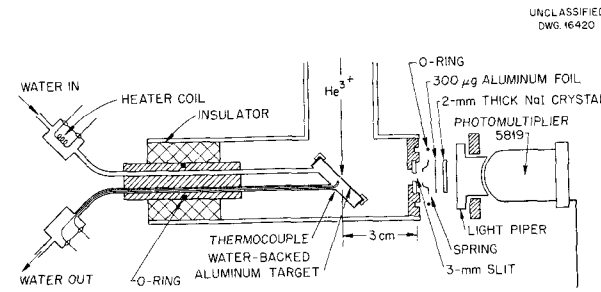

Fig. 1.3. Schematic Diagram of Target Arrangement for Studying the Energy Spectrum of Decay Products from He^3 + He^3.

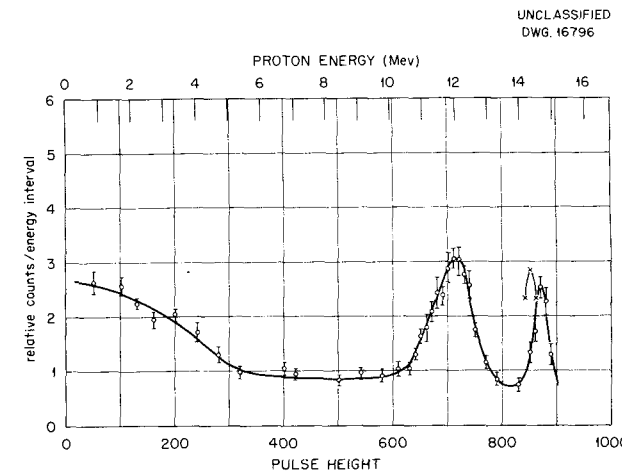

Fig. 1.4. Pulse Spectrum in Sodium Iodide of Protons from the Reactions $Li^6(He^3,H^1)Be^8$, $Li^6(He^3,He^4)Li^5$, and $Li^6(He^3,He^4,He^4)H^1$.

Lithium-6. The Li^6 target was in the form $Li_2^6SO_4$ that was mounted on an aluminum backing. A 3-mil aluminum absorber was placed between the target and the crystal to absorb all alpha particles so that the spectrum observed would be due to protons only. The reactions observed were

$$Li^6 + He^3 \longrightarrow B^{9*} \begin{cases} \nearrow Be^8 + H^1 \longrightarrow H^1 + He^4 + He^4 & (1) \\ \rightarrow Li^5 + He^4 \longrightarrow H^1 + He^4 + He^4 & (2) \\ \searrow He^4 + He^4 + H^1 & (3) \end{cases}$$

The bombarding energy of 720 kev was obtained by accelerating doubly ionized He^3 with 360 kv of accelerating voltage. The target was arranged so that deuterium-zirconium could be substituted for the Li^6 target, thus providing 14.7-Mev protons for calibration of the spectrometer. Figure 1.4 shows the proton spectrum obtained. The proton peaks at 14.6 and 12.0 Mev are the transitions to the ground state and first excited state of Be^8, respectively. The present experiment yields, for the first excited state, an excitation energy of 3.16 Mev above the ground state with a width at half maximum of 0.85 Mev. The presence of a peak at the proton energy of 3.35 Mev is doubted because recoiling Li^5 nuclei in reaction 2 will yield protons whose energies will extend to about 5.3 Mev. The flat part of the spectrum above 5.3 Mev is 15 times background and presumably arises from reaction 3, the three-body mode of decay.

The presence of only two groups of protons in this reaction is in marked contrast with other experiments leading to the formation of Be^8, for example, $B^{10}(d,\alpha)Be^8$[11] and $Li^7(d,n)Be^8$,[12] which show three and more than three groups of particles, respectively.

Helium-3. The He^3 reactions are as follows:

$$He^3 + He^3 \longrightarrow Be^{6*} \begin{cases} \nearrow Li^5 + H^1 & (a) \\ \searrow He^4 + H^1 + H^1 & (b) \end{cases}$$

The He^3 target was built up in an aluminum foil by the He^3 in the beam as was mentioned previously. Figure 1.5 shows the spectrum of protons that was obtained. The peak at pulse-height 850 results from deuterium contamination in the target that gives rise to the $He^3(d,p)He^4$ reaction; the protons from this reaction give a 14.7-Mev energy calibration and also give a measure of the instrumental resolution. The curve of Fig. 1.5 indicates that reactions (*a*) and (*b*) both occur, but more data will be required to verify the existence of the structure in the spectrum. The shape of the proton spectrum of reaction (*b*) is not known either experimentally or theoretically, and without a knowledge of the shape of this part of the spectrum there is an essential uncertainty in the position of the barely perceptible group of protons at energy 8.6 Mev. Apart from the uncertainties in the location of the maximum energy peak at 8.6 Mev owing to reaction (*b*), the value 8.6 Mev would correspond to the ground state of Li^5 being located 2.8 Mev above an alpha particle and a free proton.

Critchfield and Dodder[13] found from analysis of proton scattering on helium that either a $^2P_{1/2}$ state at 1.8 Mev or a $^2P_{3/2}$ state at 2.2 Mev is consistent with the scattering data. The value of 2.4 Mev obtained in the present experiment together with the scattering results would identify the ground state of Li^5 as $^2P_{3/2}$.

(11) L. L. Green and W. M. Gibson, *Proc. Phys. Soc. (London)* **A62**, 407 (1949).

(12) C. L. Smith and E. B. M. Murrell, *Proc. Cambridge Phil. Soc.* **35**, 298 (1939).

(13) C. L. Critchfield and D. C. Dodder, *Phys. Rev.* **76**, 602 (1949).

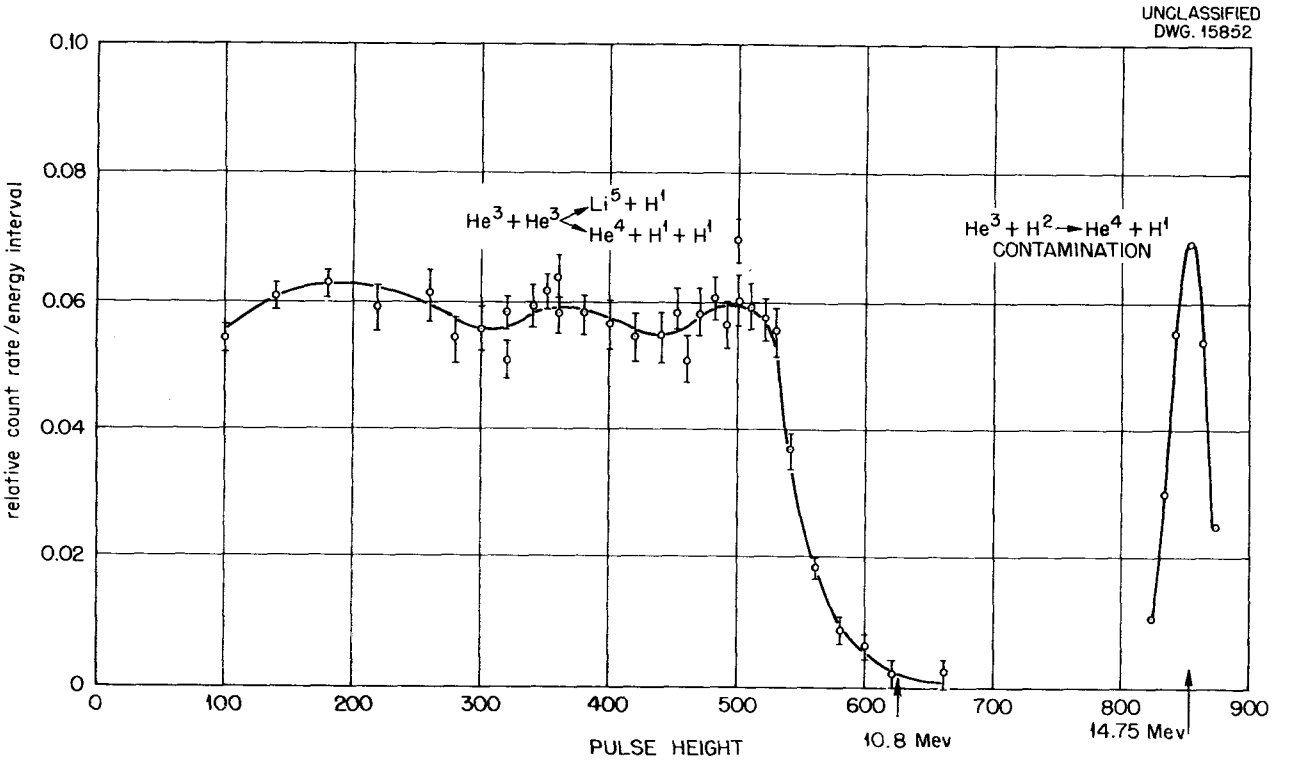

Fig. 1.5. Pulse Spectrum in Sodium Iodide of Particles from He^3 + He^3. Bombarding energy, 300 kev; 90 deg to beam; zero absorber.

A comparison of the two companion reactions, $He^3 + He^3$ and $He^3 + H^3$ (see next section), makes it possible to question whether the mode $He^3(He^3,p)Li^5$ has been observed; in contrast, the companion mode $He^3(H^3,p)He^5$ is prominent and constitutes about 10% of the transitions. Further studies will show whether the peaks of Fig. 1.5 do in fact exist.

Tritium. The H^3 reactions involved are the following:

$$He^3 + H^3 \longrightarrow Li^{6*} \begin{cases} He^4 + n + H^1 & (1) \\ He^4 + H^2 & (2) \\ He^5 + H^1 \longrightarrow He^4 + H^1 + n & (3) \\ Li^5 + n \longrightarrow He^4 + H^1 + n & (4) \end{cases}$$

The target used in this case was a thick layer of zirconium impregnated with tritium. The charged-particle spectrum obtained from these reactions is that shown in Fig. 1.6. The various parts of the spectrum are labeled to show which mode of decay is being observed. No evidence of structure could be found on this figure that would correspond to levels in He^5. Unfortunately, the expected position of a peak corresponding to the ground state of He^5 was just under, and obscured by, the line spectrum of deuterons coming from Eq. 2. An absorber, placed between the target and the counter, was used to uncover this region of the proton spectrum of Eq. 3. A deuteron will lose almost twice as much energy in an absorber as will a proton of the same energy; by virtue of this fact the peak of deuterons was shifted downscale by an aluminum absorber without a correspondingly large shift for protons of the same energy. The spectrum shown in Fig. 1.7 was obtained by repeating the pulse-height analysis with 11 mils of aluminum placed between the target and the

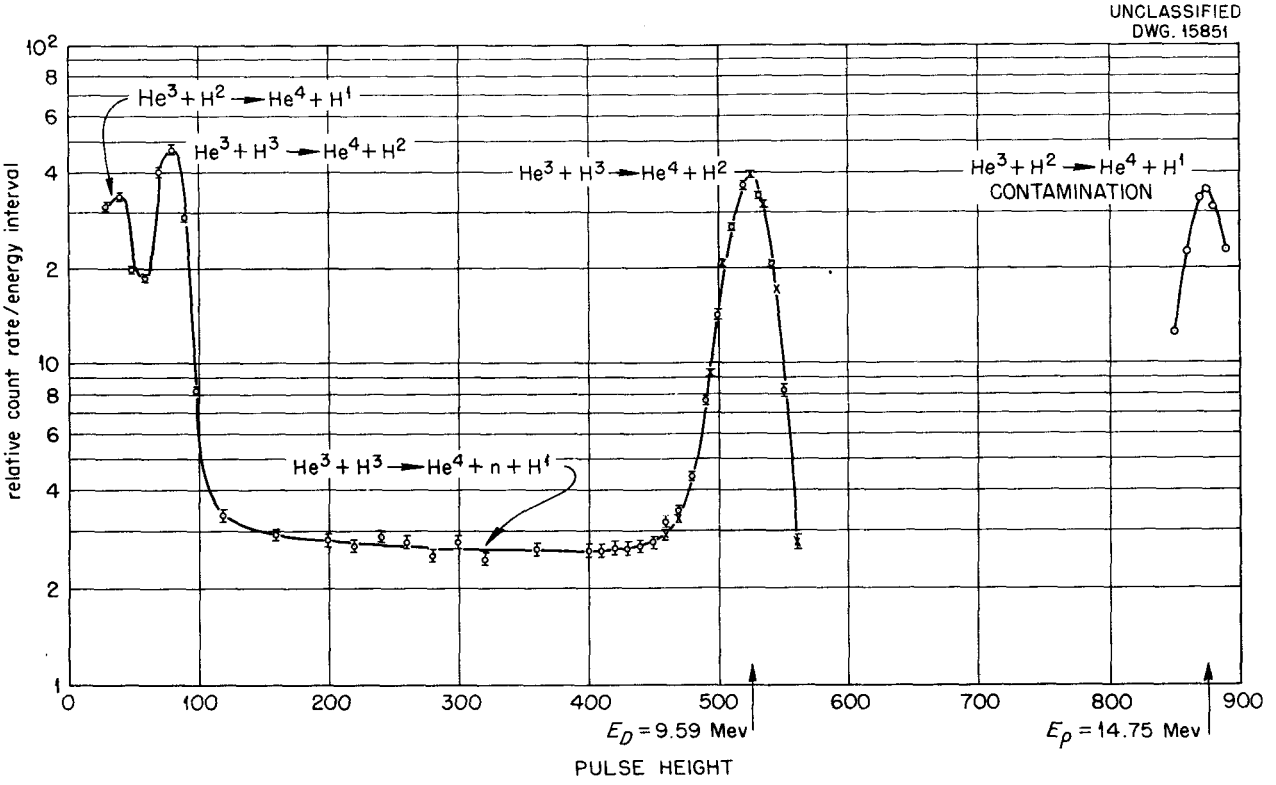

Fig. 1.6. Pulse Spectrum in Sodium Iodide of Particles from $He^3 + H^3$. Bombarding energy, 300 kev; particles passing directly into sodium iodide crystal.

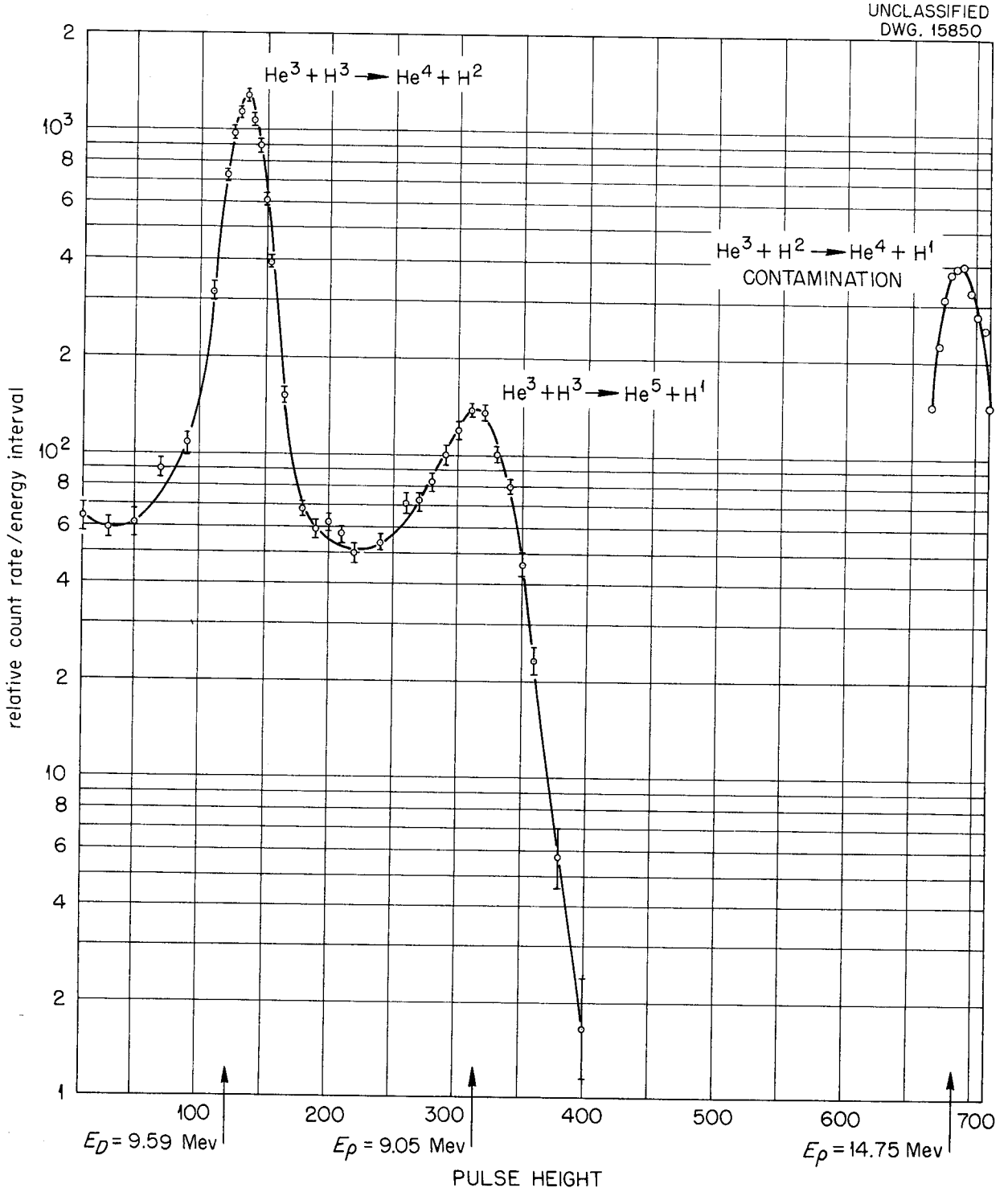

Fig. 1.7. Pulse Spectrum in Sodium Iodide of Particles from He^3 + H^3. Bombarding energy, 300 kev; particles passing through 11 mils of aluminum into sodium iodide crystal.

counter. The peak corresponding to the ground state of He^5 is clearly visible in this instance. Analysis of the data gives a value of −0.79 Mev for the binding energy of the He^5 nucleus.

It can be seen in Fig. 1.7 that the width of the He^5 peak is considerably larger than that resulting from error in instrumental resolution. Unfortunately this peak is superimposed on the spectrum of three-body breakup (Eq. 1) whose shape in this region is unknown. Since the shape of this spectrum is unknown, the resultant peak caused by He^5 alone cannot be derived from the data; for this reason no estimate can be given for the width of the He^5 ground state.

The measurement of the cross section for this reaction is almost complete and will be reported after the conclusion of some angular-distribution studies.

2. RADIOACTIVITY AND NUCLEAR ISOMERISM

GAMMA-RAY ABSORPTION AND SCATTERING

P. R. Bell D. S. Hughes[1]
R. C. Davis W. H. Jordan
C. A. Randall[1]

In much of the work with radioactive isotopes it is important to know the number of gamma rays of a given energy that are emitted per second from the source in question. In some cases it is possible to determine the absolute disintegration rate by coincidence techniques. If such a calibrated source is placed near the crystal of a scintillation counter, a measurement of the counting rate is all that is needed to determine the efficiency of the counter for the particular geometry and gamma-ray energy involved. This method has been used for determining the efficiency of a sodium iodide crystal for detecting the 1.33-Mev gamma rays from a Co^{60} source. It amounts to an indirect measurement of the absorption coefficient; the results are listed in Table 2.1 along with direct measurements that are subsequently described in this section.

A knowledge of the absorption coefficients of sodium iodide for various gamma-ray energies permits, from purely geometric considerations, a computation to be made on the efficiency of a crystal of known size when it is placed in a known position with respect to a gamma-ray source. A table of efficiencies for arbitrary values of τ (absorption coefficient) has been computed for a fixed geometry by the Mathematics Panel and is available for distribution. The major uncertainty lies in the value of the absorption coefficient. It is necessary to know the sum of the photoelectric, Compton, and pair cross sections. What is usually measured is the total cross section from which the coherent-scattering cross section must be substracted. Attempts have been made to measure the absorption cross sections and the scattering cross sections of sodium iodide for several gamma-ray energies.

[1]Summer research participant.

TABLE 2.1. GAMMA-RAY ABSORPTION COEFFICIENTS IN SODIUM IODIDE

SOURCE	GAMMA-RAY ENERGY (kev)	ABSORPTION COEFFICIENT (cm^{-1})	REMARKS
Ce^{141}	141	2.23	Measured by Bell and Heath
Hg^{203}	279	0.591	Measured by Bell and Heath
		0.6061	Measured by Hughes and Randall
Cs^{137}	661	0.275	Measured by Bell and Heath
		0.2578	Measured by Hughes and Randall, Harshaw crystals
		0.2574	Measured by Hughes and Randall, cast crystals
Zn^{65}	1.114	0.192	Measured by Bell and Heath
		0.1910 ± 0.0008	Measured by Hughes and Randall
Co^{60}	1.33	0.191	Measured by Bell and Davis, beta-gamma coincidences

The work of Bell and Heath on absorption coefficients was described in the last quarterly report.[2] The experimental arrangement has been modified somewhat, as shown in Fig. 2.1, but the procedure for analyzing the data is unchanged. The sodium iodide absorbers are surrounded with a hydrogen atmosphere to reduce the effects resulting from small-angle scattering by the atmosphere into the crystal. A lead collimator above the crystal further reduces such interference. The scintillation spectrometer measures the quantity of undegraded radiation falling on the detector for several thicknesses of absorber.

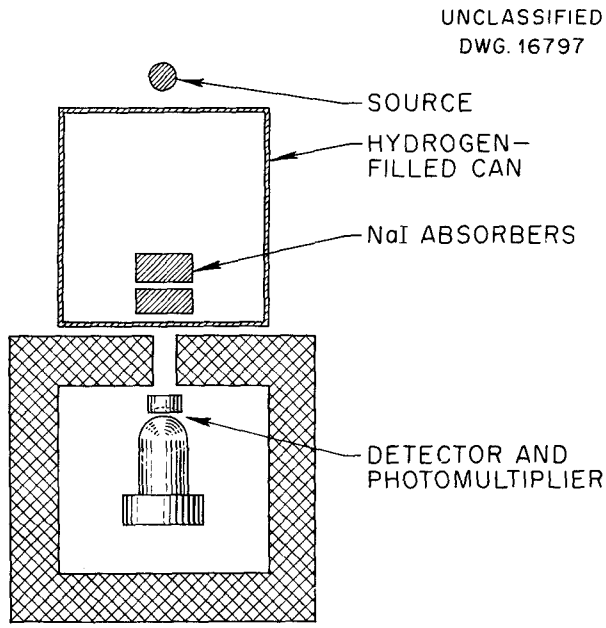

Fig. 2.1. Apparatus for Measuring Attenuation of Gamma Rays in Sodium Iodide.

The absorption coefficients obtained from these measurements are listed in Table 2.1. The earlier work of Bell and Heath is listed as well as the values obtained by Hughes and Randall with the improved arrangement described in the preceding paragraph. The data in Table 2.1 are plotted as solid dots on the graph of Fig. 2.2. The solid line in this graph was taken from the tables compiled by White[3] for the *total* cross section of

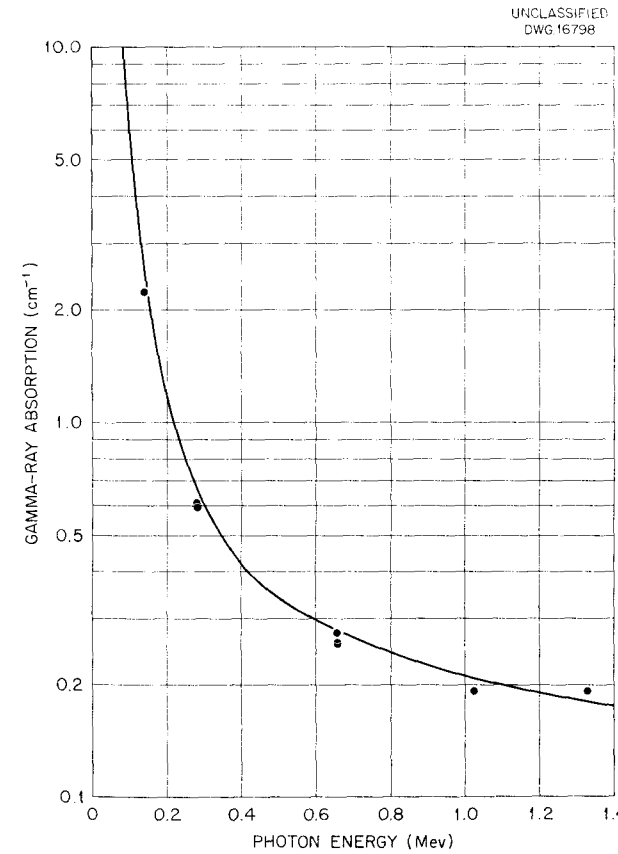

Fig. 2.2. Measured Values of Gamma-Ray Absorption Coefficients in Sodium Iodide.

sodium iodide. (A density of 3.667 was used to convert from $g \cdot cm^{-3}$ to cm^{-1}.)

The arrangement shown in Fig. 2.1 is not a "good" geometry arrangement, since photons that are scattered at small angles may still reach the detector. It is believed that the method of data analysis automatically corrects for small-angle Compton scattering; estimates as to the amount of small-angle coherent scattering have been made by D. S. Hughes. In order to compare these results with those from other laboratories, the coherent-scattering cross section must either be computed or measured, and the correction to be added to the measured values to obtain the total cross section must be estimated from the geometry of the experiment. This correction will increase the values listed in Table 2.1 by 1 or 2% but still leaves these values for total cross section several per cent below those obtained by the National Bureau of Standards. This discrepancy is a source of some concern.

[2] P. R. Bell, J. E. Richardson, and R. L. Heath, *Phys. Quar. Prog. Rep. June 20, 1952*, ORNL-1365, p. 4.

[3] G. R. White, *X-Ray Attenuation Coefficients from 10 kev to 100 Mev*, NBS-1003, p. 76 (May 13, 1952).

In the computation of crystal efficiencies, the cross section desired is the total minus the coherent-scattering cross section. Very little information exists in the literature on the coherent cross section for these energies. Compton and Allison proposed a formula for the cross section that involves the distribution of electrons in the atom. Hughes has developed an empirical expression that fits very well the numerical values for this distribution as given by the Fermi-Thomas model of the atom. This expression can be substituted into the formula and the integration can then be carried out numerically for various values of energy and atomic number. The results of these calculations, which are shown in Table 2.2 (numbers not in parentheses), express the computed amount of scattered radiation at an angle θ relative to the amount of Compton scattered radiation at the same angle.

An experiment has been performed to test the validity of the foregoing calculations. A beam of monoenergetic gamma rays was allowed to impinge upon a thin scattering disk. The radiation from the disk was measured at 90 and 135 deg with a scintillation spectrometer so that the coherent radiation could be separated from the Compton radiation emitted at the same angle. Figure 2.3 shows the pulse spectrum obtained when a lead scatterer was irradiated with the gamma rays from a Hg^{203} source. The curve for 135 deg shows the coherent-scattering peak very plainly. The height of the peak at 90 deg can be obtained by subtracting trial amounts of Hg^{203} pulse spectra to give a smooth curve. Corrections for the absorption of Compton and coherent radiation in the scatterer as well as for the relative detection efficiencies of each must be made. The observed ratio for the amount of coherent to Compton scattered radiation for a few values of energy and angle are shown by the numbers in parentheses in Table 2.2. The agreement between computed and observed ratios is not very satisfactory – both theory and experiment are believed to be at fault.

RATIO OF PEAK TO TOTAL FOR A THALLIUM-ACTIVATED SODIUM IODIDE CRYSTAL

R. L. Heath[4] P. R. Bell
R. C. Davis

A measurement of the rate of emission of gamma rays from a given source involves a knowledge of the detection efficiency and a counting of the total number of gamma rays detected (in a given time interval) by the crystal. The latter requires a plot of the entire pulse spectrum and an integration under the curve. This is readily accomplished with a monoenergetic gamma ray but is time-consuming; the process can hardly be done when a mixed gamma-ray source is used. Therefore, a sodium iodide crystal, 1½ in. in diameter and 1 in. high, and a source distance 1 cm from the crystal face have been adopted as standard. With this arrangement, the integral under the entire pulse spectrum and the integral under the photopeak portion have been measured with several monoenergetic sources. The ratio of these two integrals has been measured and is shown in Table 2.3. Figure 2.4 shows a plot of these ratios vs. energy of the gamma rays. With this curve and

[4]On loan from the American Cyanamid Co.

TABLE 2.2. RATIO OF COHERENT TO COMPTON SCATTERED RADIATION, $(d\sigma_c/d\Omega)/(d\sigma_K/d\Omega)$

Z	E	θ		
		45 deg	90 deg	135 deg
48	279	0.034	0.0082 (0.0026)	0.0049
	661	0.0032	0.00027 (0.00015)	0.00020
82	279	0.096	0.022 (0.014)	0.014 (0.030)
	661		0.0026 (0.0017)	0.00062

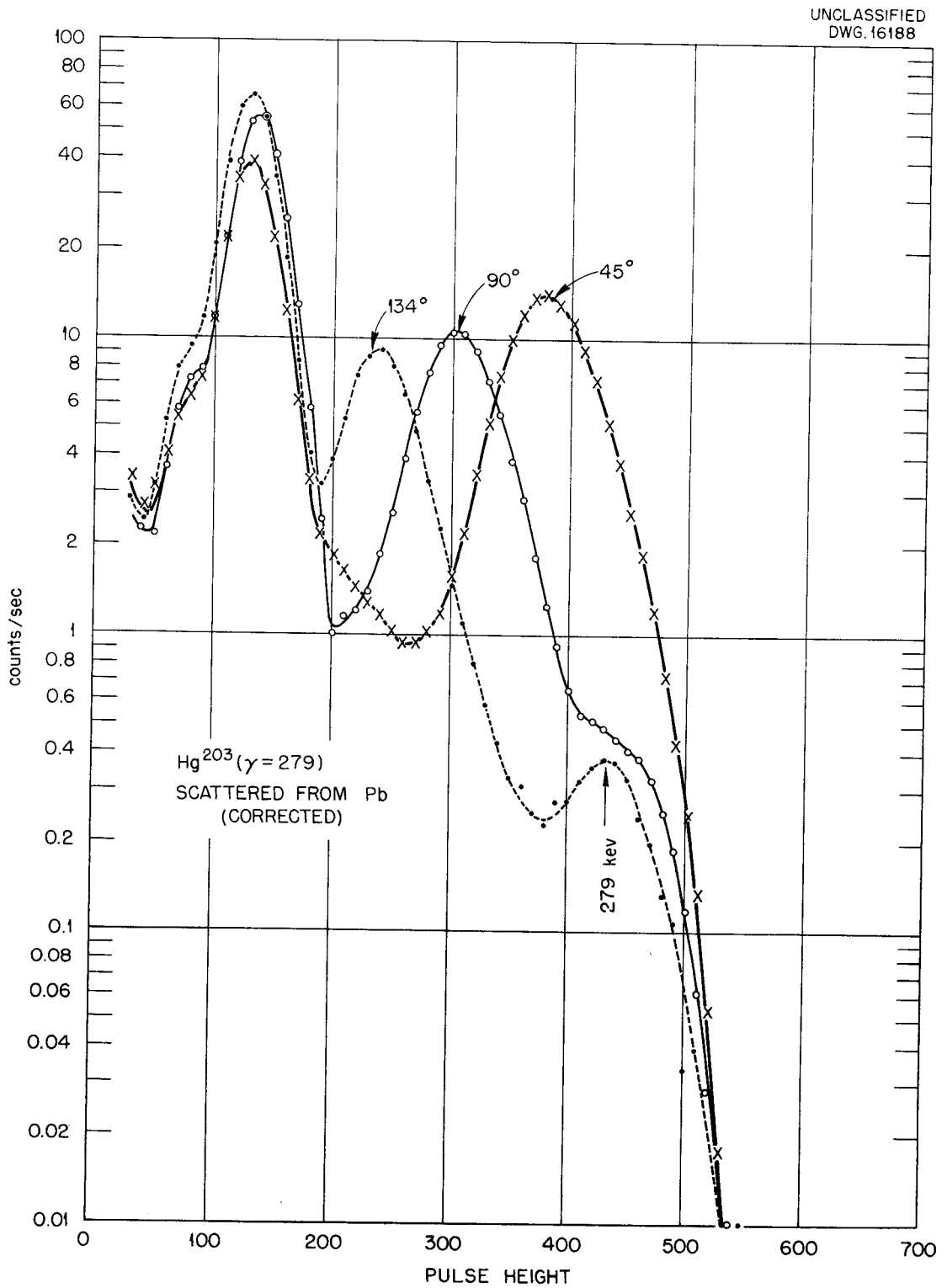

Fig. 2.3. Pulse Spectrum of Coherent-scattered Gamma Rays from Lead.

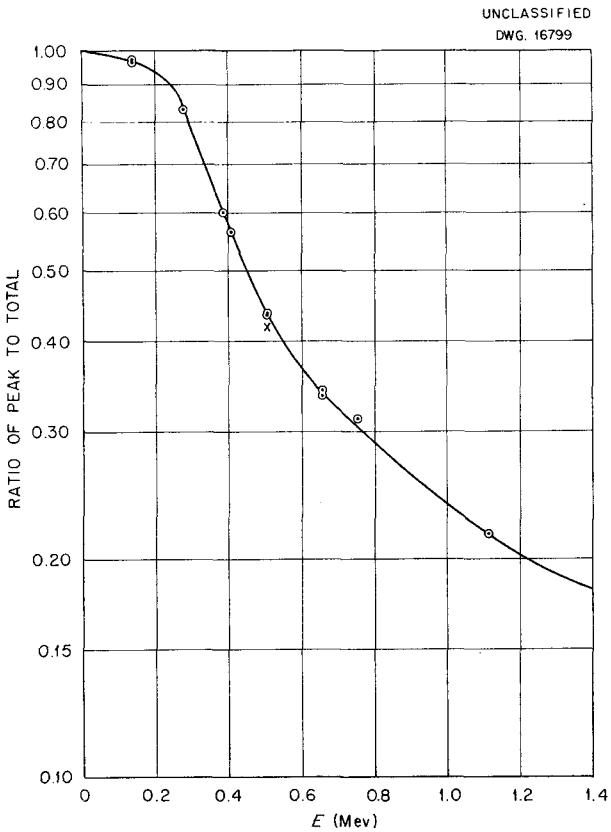

Fig. 2.4. Ratio of Integrated Photopeak of Total Counts Produced in a 1½- by 1-in. Crystal of Thallium-activated Sodium Iodide.

the standard geometry, an unknown gamma-ray intensity can be determined by measuring only the area under the photopeak.

GAMMA-GAMMA ANGULAR CORRELATIONS IN Ta^{181} AND Hf^{177}

F. K. McGowan

It was reported in the last quarterly[5] that there was an appreciable effect of the chemical state of the Hf^{181} sources on the directional angular correlation of the 132- and 481-kev gamma-ray cascades in Ta^{181}. A number of solutions of the radioactive material have been prepared with the aid of B. H. Kettelle of the Chemistry Division. Results for the directional angular-correlation anisotropy of the 132- and 481-kev gamma-ray cascades are shown in Table 2.4.

The calculated anisotropy for the sequence 1/2(*E*2)5/2(*E*2,M1)7/2 is −0.62 for $|\beta/\alpha| = 1.3$. It would appear that the disturbance of the angular correlation by the electron shell is still appreciable even with solution sources. The directional correlation function in the presence of a magnetic field caused by the electron shell can be written as

$$W(\theta) = 1 + \sum_{i=1} G_{2i} A_{2i} P_{2i} (\cos\theta) ,$$

where the influence of the shell is contained in the attenuation factor G_{2i}.[6] The attenuation becomes stronger with increasing index i and with decreasing spin of the intermediate nuclear state of the cascade. If the attenuation of the directional correlation is due to the action of the magnetic field, then a measurement of the coefficients A_2 and A_4 in the expansion

$$W(\theta) = 1 + A_2 P_2 (\cos\theta) + A_4 P_4 (\cos\theta)$$

should serve as a guide to the correctness of the foregoing sequence assignment.

A series of experiments has been performed to measure A_2 and A_4 by using a liquid source (hafnium metal taken up in 0.05 ml of HF) of Hf^{181}. A total of $N = 2.4 \times 10^6$ coincidence counts was collected with $N/2$ taken at 135 deg, $N/4$ taken at 90 deg, and $N/4$ taken at 180 degrees. The results are tabulated in Table 2.5. The coefficients a_2 and a_4 for $W(\theta)$ expanded in a power series of $\cos^2\theta$ are also tabulated. The experimental coefficients have not been corrected for the finite angular resolution of the detectors. These corrections, as a function of gamma-ray energy, are being computed by the Mathematics Panel. Inasmuch as the corrections are small, these values may be compared with the expected unperturbed directional angular correlation, where $a_2 + a_4 = -0.62$, $A_2 = -0.487$, and $A_4 = -0.0448$. The fact that A_4 is not attenuated throws some doubt on the correctness of the sequence assignment given in the preceding paragraph. The sequence 5/2(*E*2)9/2(M1,*E*2)7/2 does agree with the anisotropy of −0.38 and with the measured values of a_2 and a_4. However, this assignment fails to explain the low intensity (0.8%) of the crossover transition, 5/2 → 7/2, of 612 kev that is in competition with the 132-kev *E*2 transition.

These measurements are being continued with resolving times of approximately 10^{-8} rather than

[5] F. K. McGowan, *Phys. Quar. Prog. Rep. June 20, 1952*, ORNL-1365, p. 8.

[6] K. Alder, *Phys. Rev.* **83**, 1266 (1951).

TABLE 2.3. RATIO OF INTEGRATED COUNTS UNDER PHOTOPEAK TO TOTAL COUNTS PRODUCED IN A STANDARD CYLINDER OF THALLIUM-ACTIVATED SODIUM IODIDE

Source 1 cm from face of crystal unless noted otherwise

SOURCE	ENERGY (kev)	RATIO OF PEAK TO TOTAL	REMARKS
Ce^{141}	141	0.976 0.967	
Hg^{203}	279	0.833	
Sn^{113}	390	0.60	255-kev gamma ray was subtracted
Au^{198}	411	0.565	
Cu^{64}	511	0.437	135-kev gamma ray was subtracted
Sr^{85}	511	0.433 0.418	Source 6 cm from crystal
Cs^{137}	661	0.3365 0.335 0.3405	
Cb^{95}	758	0.313	
Zn^{65}	1.114	0.217	511-kev gamma ray was subtracted

TABLE 2.4. EFFECT OF CHEMICAL STATE OF HAFNIUM ON ANGULAR CORRELATION

FORM	ANISOTROPY
Metal	−0.06
Liquid (metal taken up in 0.100 ml of HF)	−0.38
(metal taken up in 0.300 ml of HF)	−0.38
(above source with 0.100 ml of $HClO_4 \cdot 2H_2O$ added to the solution)	−0.38
(above source 24 hr after preparation)	−0.31
(above source 48 hr after preparation)	−0.26
(above source 21 days after preparation)	−0.22
(0.300 ml of $HfOCl_2$ solution)	−0.28
(dilute HF to just take up the metal into solution)	−0.32
(Hf was extracted into a benzene layer containing TTA)	−0.12

10^{-7} second. Measurements of the anisotropy as a function of the time of emission of the 481-kev transition are being considered.

The combined correlation of the 132- with the 345-kev gamma ray and the 345- with the 135-kev gamma ray has been measured with liquid sources (HfO_2 taken up in HF) enriched in Hf^{180} before irradiation with neutrons. After correcting the measurements for the 132- and 481-kev correlation, the combined anisotropy is 0.23. The interpretation of this result is not complete.

The directional angular correlation of the gamma-ray cascade in Hf^{177} was re-examined for possible electron shell perturbation on the correlation. Measurements of the anisotropy do not differ more than 5% between a dry and a liquid source of Lu^{177}.

TABLE 2.5. EXPERIMENTAL MEASUREMENTS OF THE COEFFICIENTS A_2 AND A_4

EXPERIMENT NUMBER	ANISOTROPY $\alpha_2 + \alpha_4$	α_2	α_4	A_2	A_4
1	−0.385	−0.198	−0.187	−0.266	−0.0476
2	−0.380	−0.196	−0.184	−0.262	−0.0467
3	−0.389	−0.195	−0.194	−0.269	−0.0495
4	−0.380	−0.196	−0.184	−0.262	−0.0467

3. NEUTRON DIFFRACTION

PARAMAGNETIC SCATTERING OF NEUTRONS BY TRIVALENT IONS OF NEODYMIUM AND ERBIUM

W. C. Koehler E. O. Wollan

Neutron-diffraction measurements have been made on the oxides of the rare earths in order to study the paramagnetic scattering by the ions of the 4*f* series. Magnetic-scattering studies, up to the present time, have been confined primarily to members of the 3*d* transition group for which the orbital moments are in general strongly quenched and the scattering arises in most cases from spin only. This is the case for which the magnetic-scattering theory of Halpern and Johnson has been derived. For many rare-earth compounds, however, magnetic susceptibility data show the orbital moments to be wholly operative, and it was one of the objects of this study to obtain information on the nature of the magnetic scattering for such cases.

Not all the rare earths are amenable to study by neutron-diffraction methods, either because of the excessive thermal-neutron capture cross sections of some of them, or because of the extreme rarity of others. Fortunately, as a result of the development of column extraction techniques, it was possible to obtain sizeable quantities (several grams) of Nd_2O_3 and Pr_2O_3 from F. Spedding at Ames and of Er_2O_3 from G. E. Boyd of the ORNL Chemistry Division. The ion pair, Nd^{+++} and Er^{+++}, is particularly interesting because these ions are complementary; Nd^{+++} with three 4*f* electrons is in a $^4J_{9/2}$ state, and Er^{+++} with three vacancies in the 4*f* shell is in a $^4J_{15/2}$ state.

Measurements were made at room temperature on the hexagonal sesquioxides of praseodymium and neodymium for scattering angles from 3 to 90 deg, on the cubic form of Nd_2O_3, and on Er_2O_3 for the same angular range. From the analysis of the data, the following conclusions were reached:

1. In each case the cross section for magnetic scattering in the forward direction is in satisfactory agreement with that calculated by replacing $g_S^2\ S(S+1)$ with $g_J^2\ J(J+1)$ in the Halpern and Johnson expression for the magnetic scattering.

2. The angular dependence of the magnetic scattering is similar for Pr_2O_3 and Nd_2O_3 but markedly different for Er_2O_3. For comparison purposes the amplitude form factor for the 4*f* shell was calculated from the semiempirical screening constants given by Pauling and Sherman.[1] This electron-distribution form factor, which would apply to magnetic scattering arising from spin only, falls essentially to zero for $k \equiv (4\pi \sin\theta)/\lambda = 5.0$. For Er_2O_3 the observed magnetic-scattering amplitude has the same general character but it persists to considerable higher k values. In Nd_2O_3 and Pr_2O_3 the scattering amplitude is essentially angularly independent from $k = 0$ to $k = 3.5$, after which it falls off slowly to zero in the region of $k = 6.5$.

3. The cubic form of Nd_2O_3 was prepared to change the electrostatic field acting on the neodymium ion. Within an estimated experimental error of less than 10%, no change in the magnetic scattering was observed.

Measurements were also made on these salts at temperatures as low as 20.4°K. No coherent

[1] L. Pauling and J. Sherman, *Z. Krist.* 81, 1 (1932).

magnetic effects, suggestive of strong exchange coupling, were observed, and the diffuse scattering remained constant within experimental error. The theory of magnetic scattering of neutrons has, as was mentioned, been worked out for the case of spin only. In those cases where there are also orbital contributions, the theory becomes much more difficult.

The difference in the angular dependence of the scattering by the neodymium and erbium ions can, however, be approximately accounted for on the basis of the following considerations. Although the forward scattering is proportional to $g\sqrt{J(J+1)}$, it is, in this case, approximately equal to $L + 2S$, and hence it may be considered that the scattering amplitudes are approximately of the form $F\alpha(f_L \pm f_S)$, where the plus sign would apply to erbium and the minus sign to neodymium. The angular dependence of f_S depends on the electron distribution and can be obtained approximately from the data of Pauling and Sherman. The orbital moments on the other hand may, on a classical basis, be considered as distributed over the area of the electronic orbit, and hence the form factor for orbital scattering will persist to larger scattering angles than for spin. A reasonable estimate of f_L on this basis, when combined with the properly normalized value for f_S, leads to an angular dependence of the scattering by neodymium and erbium that is in good accord with the experiments.

A more rigorous treatment of this problem has been made by G. T. Trammell, who has calculated the first two terms in a series expansion of the magnetic form factor for neodymium and erbium (cf. "Theoretical Physics," this report). An extension of the theory will, however, be required to permit a good comparison with the results of the experiments to be made.

4. NEUTRON CROSS SECTIONS

TOTAL CROSS-SECTION MEASUREMENTS WITH TIME-OF-FLIGHT SPECTROMETER

G. S. Pawlicki E. C. Smith
P. E. F. Thurlow

Cross-section measurements with the time-of-flight spectrometer were made on copper and thorium with resolutions of 0.55 and 0.50 μsec/m, respectively. Resolutions quoted henceforth will be the full width at half maximum of the resolution function.

Copper. The transmission of a 22.43 g/cm^2 sample of copper metal is presented in Fig. 4.1. The resonances at 1.6 and 2.6 μsec/m correspond to energies of 2200 and 720 volts, respectively. The results are in agreement with those published by the Harwell group.[1]

Thorium. The results of a measurement of the transmission of a 10.14 g/cm^2 sample of ThO_2 are shown in Fig. 4.2. The data indicate resonances at 23, 35, 71, 130, 260, and 870 ev.

[1] *Neutron Cross Sections*, AECU-2040 (May 15, 1952).

PILE-OSCILLATOR MEASUREMENTS OF STABLE-ISOTOPE CROSS SECTIONS

H. Pomerance

The thermal-neutron cross section of scandium was remeasured with the pile oscillator; the value of 11.8 barns that had been obtained previously was found to be in error. The recently obtained value of 23 barns (±5%) agrees with the work of others, including Littler and Lockett of Harwell, who determined the cross section to be 24 barns and suggested that the difference be investigated. The activation cross section was measured by W. S. Lyon of the Analytical Chemistry Division, whose first value of 23 barns (±20% because of an uncertain sample weight) is in agreement with the value of 22 barns found by Seren *et al.* in 1945. No reason for the error in the previous measurement can be found, except possibly a mistake in using gross weights instead of net weights for the samples.

Two and one-half curies of Ac^{227} recently became available in the form of the oxide. It was placed in a quartz tube that in turn was sealed and placed in a bismuth cylinder. The thermal-neutron capture cross section was measured to be 500 ± 35

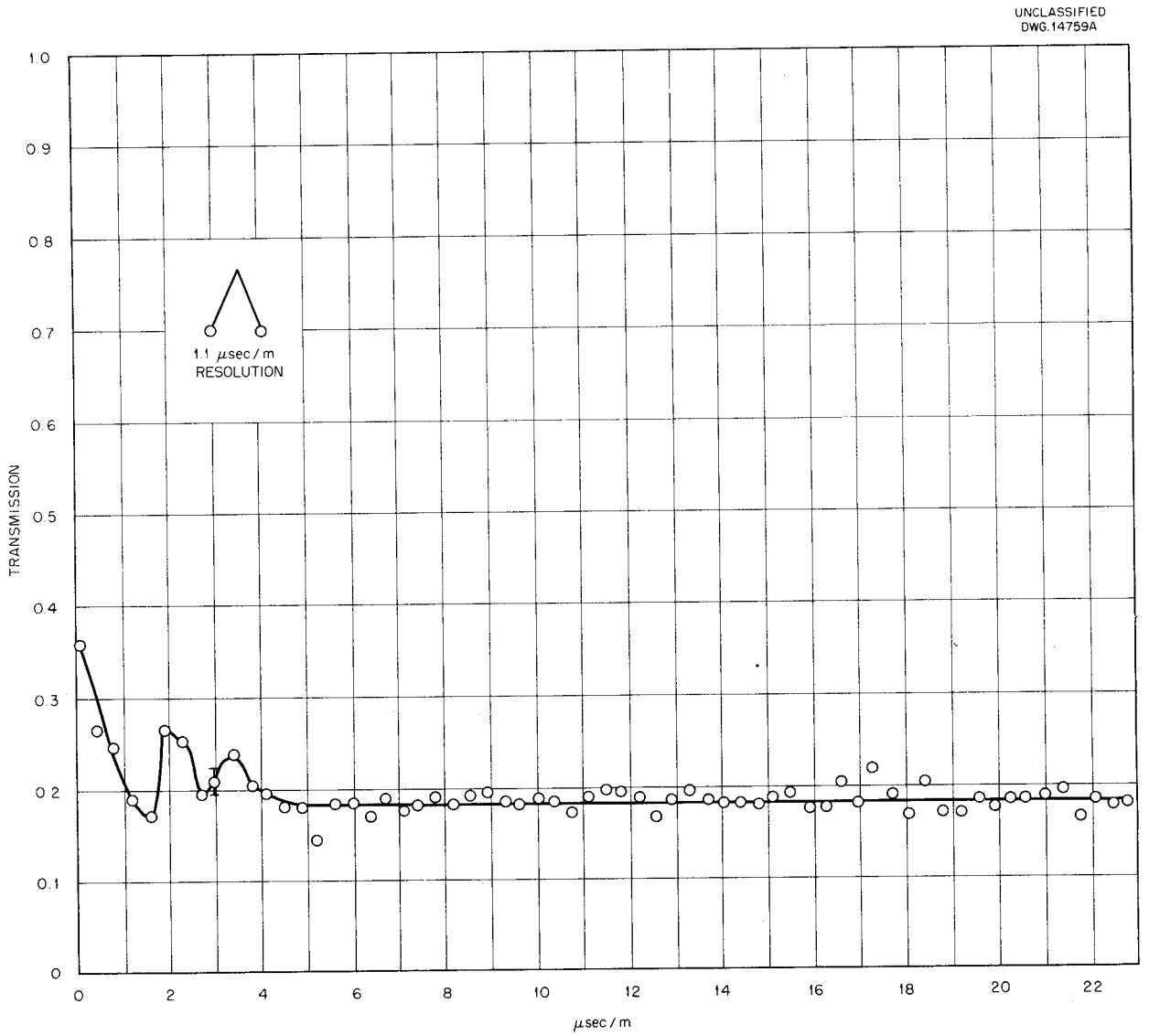

Fig. 4.1. Transmission of Copper Obtained by Using a 22.43 g/cm^2 Sample.

barns. The uncertainties are estimated to be: (1) 5% for the pile oscillator, (2) 5% for the half life of 22 years used to convert the calorimetric measurement to the number of actinium atoms, (3) 1 or 2% for mismatch of the true containers and the dummy containers.

The oscillator has been used for service analyses of various materials, principally stainless steels.

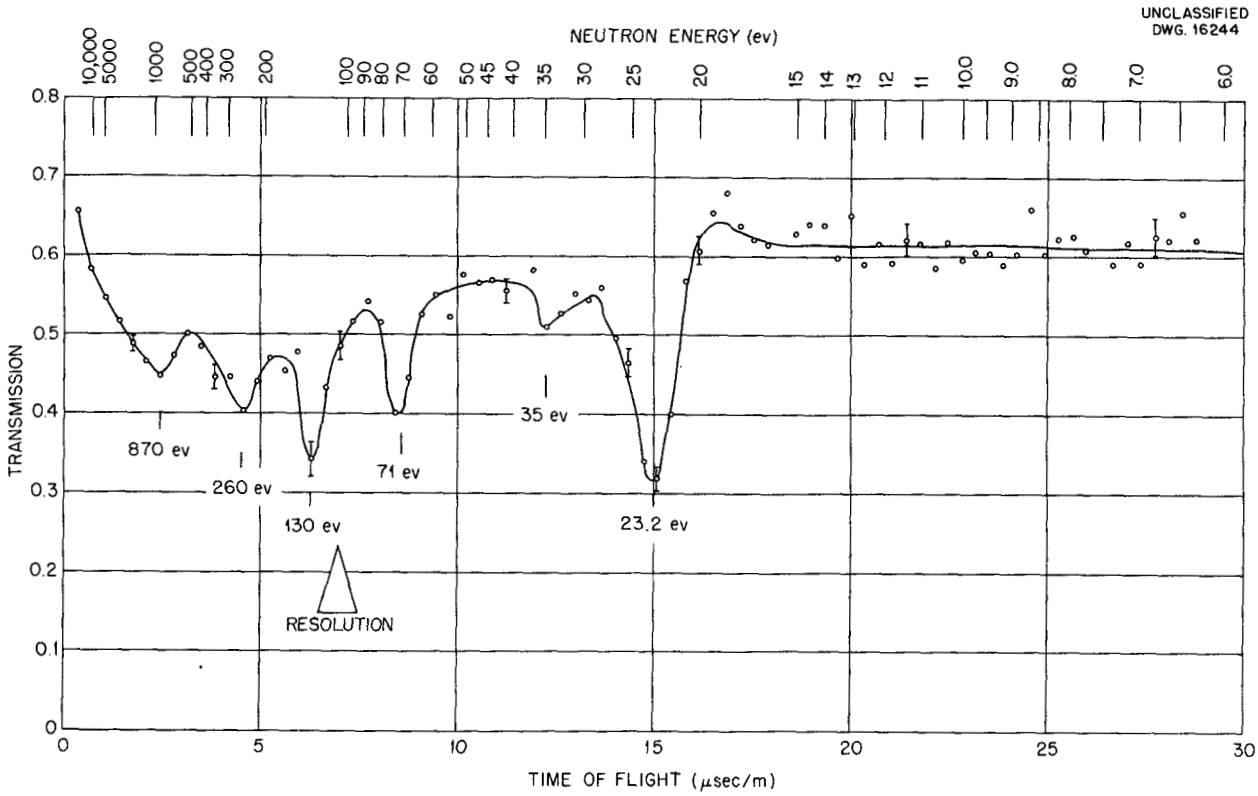

Fig. 4.2. Transmission of ThO_2 Obtained by Using a 10.14 g/cm^2 Sample.

5. THEORETICAL PHYSICS

AUGER EFFECT

M. E. Rose G. Goertzel[1]

The need for an adequate calculation of the Auger effect has existed for several years. Such calculations, if done with sufficient accuracy, could be used to determine from auxiliary experimental data the number of *K*- or *L*-shell vacancies formed in nuclear transitions and, hence, the internal-conversion coefficient. Applications can also be made to experiments involving capture of orbital electrons.

The existing calculations are, with one exception, nonrelativistic, and it is known from the one exception, which is a relativistic calculation made with the use of Slater screening constants,[2] that this approximation can lead to large errors for elements as heavy as gold. However, these calculations are far from being complete. With a *K* hole, only $L_I L_I$, $L_I L_{II}$, and $L_I L_{III}$ initial states were considered, and in the $L_I L_{III}$ case a particular final state was omitted.

The calculation for a *K* hole has been set up for the six *L*-shell initial states. The procedure for calculation would follow the methods used in the calculation of the *L*-shell internal conversion. This involves computation, for each *Z*, of the *K*- and *L*-shell bound-state wave functions and the appropriate continuum wave functions in each case

[1] Summer visitor from New York University.

[2] H. S. W. Massey and E. H. S. Burhop, *Proc. Roy. Soc. (London)* **A153**, 661 (1936).

from the relativistic central-field, Dirac wave equation. The screening is represented by a Thomas-Fermi potential with exchange. Much of this work has already been done on the SEAC for the *L*-shell internal-conversion problem. In fact, from a consideration of the calculations, the Auger effect is the natural extension of the internal-conversion process. (The Auger effect differs from the internal-conversion process only in that the exclusion principle must be incorporated, and the "nucleus" is no longer a point, but is indefinitely extended.)

Plans have been made to examine the higher shells to include *L*-*M* and *M*-*M* transitions. Then, with a comparatively straightforward calculation of the x-ray emission, the fluorescent yield can be obtained.

QUANTUM ELECTRODYNAMICS

T. A. Welton

The work on quantum electrodynamics previously reported has been continued with the hope of making possible an experimental check of the assumptions involved. When the internal consistency is considered, it is evident that a completely satisfactory positron theory comparable to the parameterized single-particle theory previously described has not yet been found. The point has, in fact, been reached where further theoretical work is likely to be fruitless without experimental guidance. The experiments that could possibly be used are described as follows:

1. The level shift in hydrogen, deuterium, and ionized helium. This work has been done to sufficient accuracy by Lamb and co-workers.
2. The scattering of x rays from a nuclear coulomb field (Delbruck scattering). This experiment is apparently being carefully done by R. R. Wilson of Cornell University, but no results are yet available.
3. The scattering of low-energy (below the energy at which nuclear scattering appears) protons or alpha particles from light nuclei. This work is apparently not in progress; some of the required numbers will be presented later in this section.

The availability of the level-shift results is counterbalanced by the fact that the calculated result is a sum of two contributions, each uncertain, so that a unique conclusion is difficult to reach. The two contributions are the electrodynamic shift (about 1080 megacycles/sec) and the positron shift (–27 megacycles/sec). The electrodynamic shift must unfortunately be considered sufficiently ambiguous to prevent a clear-cut identification of the positron shift. The reason for this is that at least two different procedures exist for calculating the electrodynamic shift. The first procedure has recently been independently carried out by Baranger and by Schwinger and Karplus. Their results coincide, and satisfactory agreement with experiment is obtained by adding in the negative positron shift.

The other available procedure is that of the parameterized single-particle theory previously described. No numerical result has yet been obtained, but some preliminary observations follow:

1. The usual g-factor change ($\alpha/2\pi$) follows from this formalism.
2. The electrodynamic level shift is grossly correct, in that the term proportional to the expectation value of the Laplacian of the atomic potential and the diverging for soft quanta agrees with previous calculations.
3. The level shift does not agree in detail with the foregoing results, and a calculation of this detailed difference is being attempted. It seems perfectly possible that this difference may be as large in magnitude as the positron shift.

By taking into account the foregoing observations, it seems desirable to perform a test of the positron effect alone. The Delbruck scattering does not check this point precisely, and some calculation has therefore been done to determine what alterations in charged-particle scattering would result from the positron effect. This effect manifests itself as a spreading-out of part of the nuclear charge over a region that is roughly a Compton wavelength in radius. Since this distance is large compared with the range of nuclear forces, yet small compared with the Bohr radius, it should be possible to study the positron-induced deviation from the coulomb field by measuring the ratio of actual scattering to Rutherford scattering over a region of energy and angle such that neither screening nor nuclear scattering plays any role.

For simplicity, it may be assumed that protons are incident on protons with an energy sufficiently low that no partial wave undergoes an appreciable nuclear phase shift, and only the $l = 0$ wave will be shifted by the positron effect. The alteration of the coulomb potential by the positron effect is

quite weak, and a perturbation calculation should therefore be valid. The additional S-wave phase shift is:

$$\delta = -\frac{Mk}{\hbar^2}\int_0^\infty r^2\,dr\,L^2(r)\,\delta V(r)\ , \qquad (1)$$

where

M = proton mass,
k = wave number for relative motion,
$L^2(r)$ = square of appropriately normalized, regular coulomb S-wave function,
$\delta V(r)$ = alteration in potential owing to positron effect.

For small k (small barrier penetration), L^2 is given by

$$L^2(r) = \frac{2\pi\eta}{e^{2\pi\eta}-1}\,4\left[\frac{J_1\left(i\sqrt{\frac{8r}{a}}\right)}{i\sqrt{\frac{8r}{a}}}\right]^2\ , \qquad (2)$$

where $a = 2\hbar^2/M\,e^2$ and $\eta = 1/ka$ over the range of r where the integrand of Eq. 1 is important. The alteration in the potential is given by

$$\delta V(r) = \frac{a}{3\pi}\frac{e^2}{r}\int_1^\infty \frac{ds}{s^2}(s^2-1)^{1/2}\,e^{-2sKr}\left(2+\frac{1}{s^2}\right)\ , \qquad (3)$$

where $K = mc/\hbar$ and m = electron mass. For the specific problem of interest, both Eqs. 2 and 3 can be approximated by asymptotic expansions, and Eq. 1 becomes

$$\delta = -\frac{a}{16\pi}\,\frac{\sqrt{2\pi}}{e^{2\pi\eta}-1}\int_{(0)}^\infty \frac{dx}{x^4}\,e^{-x^2}\,e^{\beta x}\ , \qquad (4)$$

in which $\beta = 4/\sqrt{Ka} = 10.38$, where the lower limit designated (0) is only approximately defined (it is roughly unity), with the apparent divergence arising from the use of the asymptotic expansions to zero value of the argument. The treatment will be valid providing the bulk of the integral arises from $x \gg 1$, as it does in the present case. The integrand of Eq. 4 has a saddle-point at $x = \beta/2$, and an approximate value for Eq. 4 is then given by

$$\delta = \frac{-a\sqrt{2}}{\beta^4(e^{2\pi\eta}-1)}\,e^{\beta^2/4}\ . \qquad (5)$$

This expression for δ increases with energy ($\eta \simeq 1/\sqrt{E}$, E = bombarding energy in Mev) and reaches a unity value at something less than 10 kv. Beyond this point a perturbation approach is presumably invalid, and the required work has not yet been done. A rough expression for the predicted fractional correction to the cross section at large angles is $2\delta/\eta$, which is already unity at 10 kv.

It therefore seems possible to obtain good experimental evidence on the existence or nonexistence of the positron effect by such an experiment.

NUCLEAR THREE-BODY PROBLEM

A. Simon

The separation of the angular dependence in the wave equation has been studied with the intention of setting up the nuclear three-body problem for machine computation. The result is the replacement of a set of coupled partial-differential equations in six independent variables by a set of equations in three variables. The remaining three variables are the interparticle distances. The result checks with that recently obtained by Majumdar.[3]

The resulting equation can be handled by a digital computer in several ways, and it is planned to schedule sample calculations in order to make some decision from among the available methods. The first objective is to develop a flexible and reliable method for studying the effects of various nuclear-force assumptions on the binding energies.

SCATTERING OF SLOW NEUTRONS BY ATOMS WITH NONZERO ORBITAL MOMENTS

G. T. Trammell

The magnetic scattering of neutrons by paramagnetic rare-earth ions has been studied experimentally at this laboratory by Koehler and Wollan (cf. "Neutron Diffraction," this report). The electrons that are responsible for the scattering are those in the 4f shell. The orbital moments are

[3] S. D. Majumdar, *Z. Physik* 131, 528 (1952).

not quenched by the crystalline fields and are, for these crystals at room temperatures, free to orient themselves at random with respect to each other. The wavelength of the neutrons involved is approximately 1 Å.

The problem of obtaining a theoretical expression for the scattering is quite complicated if there are more than one or two electrons with nonzero orbital moments contributing to the scattering. In particular, the scattering by Nd^{+++} (three 4f electrons with $L = 6$, $S = 3/2$, and $J = 9/2$) is of interest here. The corresponding expression that is valid for S electrons, or for electrons for which the orbital moments are quenched because of crystalline fields, has been given by Halpern and Johnson.[4]

$$S_{if} = g_N \frac{e}{c} (\chi_f | \vec{S}_N | \chi_i) \cdot \frac{\vec{k}}{k^2} \times (\psi_f | \sum_n \vec{\alpha}_n e^{i\vec{k}\cdot\vec{r}_n} | \psi_i) , \quad (1)$$

where g_N is the gyromagnetic ratio for the neutron, $\vec{S}_N$ is the spin of the neutron, $\vec{\alpha}_n$ is the Dirac velocity operator for the nth electron, and the sum is for the atomic electrons. The differential cross section involves just the absolute square of Eq. 1.

Upon making the Pauli nonrelativistic approximation, the following expression is obtained:

$$\begin{aligned} - \frac{e}{c} (\psi_f | \sum_n \vec{\alpha}_n e^{ik\cdot r_n} | \psi_i) &\doteq \frac{e}{c} (\psi_f | \sum_n \frac{1}{2m} (\vec{p}_n e^{ik\cdot r_n} + e^{ik\cdot r_n} \vec{p}_n) + \frac{1}{m} \vec{k} \times \vec{S}_n e^{ik\cdot r_n} | \psi_i) \\ &\doteq \frac{e}{2mc} \vec{k} \times (\psi_f | \sum_n \vec{L}_n f(k\cdot r_n) f(k\cdot r_n) \vec{L}_n + 2\vec{S}_n e^{ik\cdot r_n} | \psi_i) , \end{aligned} \quad (2)$$

The expressions developed in the following material make it possible to predict the scattering so long as

$$\overline{r^2_{atom}} \frac{\sin^2 \theta_{scattering}}{\lambda^2_{neutron}}$$

is small. Work is in progress on a more general treatment of this problem.

Since the neutron-electron magnetic interaction is quite small, the Born approximation is used in the following treatment.

If the neutron is assumed initially to be in the plane wave state with momentum p_i and spin state χ_i and the atom to be in the unperturbed electronic state ψ_i, then the amplitude for the neutron to make a transition to a state with momentum $\vec{p}_i + \hbar\vec{k}$ and spin state χ_f and for the atom to make a transition to the state ψ_f is[4,5]

where

$$\overline{f(k\cdot r)} = \sum_0^\infty \frac{(ik\cdot r)^n}{(n+2)n!} , \quad (3)$$

and $\vec{S}_n$ and $\vec{L}_n$ are respectively the spin and orbital angular momentum operators for the nth electron.

Aside from some constant factors, Eq. 1 may be written as

$$S_{if} = (\chi_f \psi_f | (\vec{e}\cdot\vec{\mu})(\vec{e}\cdot\vec{S}_n) - \vec{S}_n \cdot \vec{\mu} | \chi_i \psi_i) , \quad (4)$$

where

$$\vec{\mu} = \sum_n \left\{ \vec{L}_n f(k\cdot r_n) + f(k\cdot r_n) \vec{L}_n + 2\vec{S}_n e^{ik\cdot r_n} \right\} \quad (5)$$

and $\vec{e} = \vec{k}/k$. What is of interest here is

$$\sum_{\chi_i, \chi_f, \psi_i, \psi_f} |S_{if}|^2 ,$$

and from Eq. 4 the expression

$$\sum_{\chi_i, \chi_f} |S_{if}|^2 = (\psi_f | \vec{\mu} | \psi_i) \cdot (\psi_i | \vec{\mu} | \psi_f) - (\psi_f | \vec{\mu}\cdot\vec{e} | \psi_i)(\psi_i | \vec{\mu}\cdot\vec{e} | \psi_f) \quad (6)$$

(4) O. Halpern and M. H. Johnson, *Phys. Rev.* **55**, 898 (1939); see also, J. S. Schwinger, *Phys. Rev.* **51**, 544 (1937).

(5) The assumption is made that the neutron has insufficient energy to excite the atom.

is obtained, except for some factors of K. In Eq. 6 the assumption has been made that the incoming neutron beam is unpolarized. A summation over the initial and final states of the atom and the assumption that the atoms are oriented at random gives the equation

$$\sum_{\psi_i,\psi_f,\chi_i,\chi_f} |S_{if}|^2 = 2 \sum_{\psi_i,\psi_f} (\psi_f|\vec{\mu}\cdot\vec{e}'|\psi_i)\,(\psi_i|\vec{\mu}\cdot\vec{e}'|\psi_f)\,, \quad (7)$$

where $\vec{e}'$ is some unit vector perpendicular to $\vec{k}$.

quantum numbers and that the neutron has insufficient energy to excite the atom to a state with a different set of these quantum numbers. With this assumption the various states ψ_i and ψ_f, over which a sum is to be made, are completely specified by their value of some component of J, for example, J_z, and it is further assumed that the energy does not depend on this value.

Upon substitution of Eq. 8 into Eq. 6 and with the neglection of terms containing k^4, it is possible to obtain

$$\begin{aligned}
\frac{1}{2}\sum_{if}|S_{if}|^2 &= \sum_{if}|(\psi_f|\sum_n L_{nz} + 2S_{nz}|\psi_i)|^2 \\
&\quad - \frac{k^2}{2}\sum_{if}(\psi_f|\sum_n L_{nz} + 2S_{nz}|\psi_i)\,(\psi_i|\sum_n L_{nz}x_n^2 + x_n^2L_{nz} + 8S_{nz}x_n^2|\psi_f) \\
&\quad - \frac{k^2}{2}\sum_{if}(\psi_i|\sum_n L_{nz} + 2S_{nz}|\psi_f)\,(\psi_f|\sum_n L_{nz}x_n^2 + x_n^2L_{nz} + 8S_{nz}x_n^2|\psi_i) \qquad (9) \\
&= \sum_{M=J}^{-J}|(M|\sum_n L_{nz} + 2S_{nz}|M)|^2 \\
&\quad - k^2\overline{r^2}\sum_{M=J}^{-J}(M|\sum_n L_{nz} + 2S_{nz}|M)\,(M|\sum_n L_{nz}\left(1 - \frac{z_n^2}{r_n^2}\right) \\
&\quad + 4S_{nz}\left(1 - \frac{z_n^2}{r_n^2}\right)|M)\,, \qquad (10)
\end{aligned}$$

Aside from the inclusion in $\vec{\mu}$ of the effect of the orbital currents, the development up to this point is essentially the same as that of Halpern and Johnson.[4]

The expansion of the right side of Eq. 5 in powers of k^2 gives

$$\begin{aligned}
(\psi_f|\vec{\mu}\cdot\vec{e}'|\psi_i) &= (\psi_f|\sum_n (L_{nz} + 2S_{nz}) \\
&\quad - \frac{k^2}{2}(L_{nz}x_n^2 + x_n^2L_{nz} + 8S_{nz}x_n^2) \\
&\quad + k^4(\ldots)\ldots|\psi_i)\,, \qquad (8)
\end{aligned}$$

where $\vec{e}$ has been taken to be the x direction and $\vec{e}'$ the z direction. The small-angle approximation is made by neglecting terms in Eq. 8 involving powers of k higher than k^2.

It is assumed that all the atoms of the assembly have the same values of S^2, L^2, J^2, and radial

where (in Eq. 10) $|M)$ indicates an eigenstate of J_z with an eigenvalue of M and $\overline{r^2} = (\psi|r_i^2|\psi)$.

To evaluate Eq. 10, use is made of the following theorem: If T_i and J_j (i = 1, 2, 3) are vector operators, and if $[T_i, J_i] = 0$ (no sum intended), then for the states that are simultaneous eigenstates of some component of $\vec{J}$, for example, J_k, and a sufficient number of other operators to completely specify the state, coefficients a, b, c, ... can be found such that

$$\begin{aligned}
&(\alpha,M'|T - aJ|\alpha,M) = 0\,, \\
&(\alpha,M'|T_iT_i - b\delta_{ij} - cJ_iJ_j - dJ_jJ_i|\alpha,M) = 0\,, \\
&(\alpha,M'|T_iT_jT_k - e_{ijk} - f\delta_{ij}J_k - g\delta_{ik}J_j \qquad (11) \\
&\quad - h\delta_{jk}J_i - iJ_iJ_jJ_k - jJ_jJ_iJ_k - kJ_iJ_kJ_j \\
&\quad - lJ_jJ_kJ_i - mJ_kJ_iJ_j - nJ_kJ_jJ_i|\alpha,M) = 0\,,
\end{aligned}$$

etc., where $|a,M)$ represents a state with eigenvalue M for J_k and eigenvalues represented by a for the other operators necessary to complete the specification of the state, and the numbers a, b, c, ... are functions of a, not of M. In the following material the relations of Eq. 11 will sometimes be written symbolically as operator relations, thus: $\vec{T} = a\vec{J}$, but it is understood that this is only true for those elements of the matrix representation of the operators which refer to the same value of a. This theorem is known from group theory (Wigner-Eckart theorem).

To evaluate the first term on the right side of Eq. 10, use is made of

$$\begin{aligned} \sum_n \vec{L}_n + 2\vec{S}_n &= a\vec{J} \ , \\ \vec{J}\cdot\vec{J} + \vec{S}\cdot\vec{J} &= a\vec{J}\cdot\vec{J} \ , \\ \therefore \sum_n L_{nz} + 2S_{nz} &= \frac{J^2 + \vec{S}\cdot\vec{J}}{J^2} J_z \ . \end{aligned} \tag{12}$$

Since it is assumed that the atoms are in eigenstates of J^2, L^2, S^2, L_n^2, S_n^2, all scalar quantities appearing in Eqs. 12 to 15 are known.

In order to write $\sum_n L_{zn}^3$ and $\sum_n S_{zn} L_{zn}^2$ (which result from the substitution of Eqs. 12 to 15 in Eq. 10) in terms of L_z and S_z (and eventually in terms of J_z) it must be known how the individual $\vec{L}_n$'s are coupled to give $\vec{L}$, and how $\vec{S}_n$'s give $\vec{S}$. Russel-Saunders coupling, with L^2 and S^2 good quantum numbers, has been assumed. It is further assumed that Hund's rule gives the ground state of the atom: the q electrons have their spins aligned to give the maximum S^2 consistent with the Pauli principle, the L_n's then add to give the maximum L^2 consistent with this S^2, and the L and S are then coupled such that $L \cdot S$ is as small as possible if $q < 2L_n + 1$ and as large as possible if $q > 2L_n + 1$. If the shell is more than half full ($q < 2L_n + 1$), it is convenient to replace it by a shell containing $2(2L_n + 1) - q$ electrons, and in the material that follows it is understood that this is done.

With these assumptions it is easy to show that

$$\sum_{n=1}^{q} L_{nz}^3 = \frac{|L|^3 (3l^2 - 1) - (3L^2 - 1)\,\phi_3(l,q)}{5|L|^3 - (3L^2 - 1)\,|L|} L_z + \frac{|L|\,(3l^2 - 1) - 5\phi_3(l,q)}{|L|\,(3L^2 - 1) - 5|L|^3} L_z^3 \ , \tag{16}$$

For the evaluation of the second term on the right side of Eq. 10, use is made of

$$L_{nz} = \frac{\vec{L}\cdot\vec{J}}{J^2} J_z \ , \tag{13}$$

$$S_{nz} = \frac{\vec{S}\cdot\vec{J}}{J^2} J_z \ , \tag{14}$$

where

$$\phi_3(l,q) = \sum_{m=0}^{q-1} (l - m)^3$$

and l is the orbital moment of each of the q electrons.

$$\begin{aligned} \left(\frac{x_i}{r}\frac{x_j}{r} - \frac{1}{3}\delta_{ij}\right) &= b\left(L_iL_j + L_jL_i - \frac{2}{3}L^2\delta_{ij}\right) \ , \\ \frac{x_i}{r}\frac{r}{r}\cdot L - \frac{1}{3}L_i &= b\left(L_iL^2 + (L^2 - 1)L_i - \frac{2}{3}L^2L_i\right) \ , \\ \therefore \quad b &= -\frac{1}{4L^2 - 3} \ , \\ \therefore \quad \frac{z_n^2}{r_n^2} &= \frac{2L_n^2 - 1}{4L_n^2 - 3} - \frac{2L_{nz}^2}{4L_n^2 - 3} \ . \end{aligned} \tag{15}$$

$$\sum_{n=1}^{q} S_{nz} L_{nz}^2 = \frac{\frac{1}{q} S_z}{3\left[3|L|^2 - L^2\right]} \left\{ q l^2 \left[3|L|^2 - L^2\right] - L^2 \left[3\phi_2(l,q) - q l^2\right] + 3\left[3\phi_2(l,q) - q l^2\right] L_z^2 \right\}, \quad (17)$$

where

$$\phi_2(l,q) = \sum_{m=0}^{q-1} (l - m)^2 .$$

In Eq. 17, S_z may be replaced by $(J_z - L_z)$ and then all that remains to be done is to express L_z^2 and L_z^3 in terms of J_z. Straightforward algebra yields

$$L_z^2 = \frac{1}{3}\left[L^2 - 3\,\frac{L\cdot J\,(2L\cdot J - 1) - \frac{2}{3} L^2 J^2}{J^2 - 3}\right] + 3\,\frac{L\cdot J\,(2L\cdot J - 1) - \frac{2}{3} L^2 J^2}{(J^2 - 3)\,J^2}\, J_z^2 , \quad (18)$$

$$L_z^3 = \frac{1}{10}\left[\frac{L\cdot J\,(6L^2 - 2)}{J^2} - (6J^2 - 2)\,\chi\right] J_z + \chi J_z^3 , \quad (19)$$

where

$$\chi = \left\{ 2L\cdot J\left[3(L\cdot J)^2 - 6(L\cdot J) + 2\right] + 3L^2J^2 - \frac{2}{5}(L\cdot J)(3J^2 - 1)(3L^2 - 1)\right\} \cdot \left\{ 2J^2\left[\left(3J^4 - \frac{9}{2}J^2 + 2\right) - \frac{1}{5}(3J^2 - 1)\right]\right\}^{-1} . \quad (20)$$

The quantities $A(J^2, L^2, S^2, l^2, q)$ and $B(J^2, L^2, S^2, l^2, q)$ in the equality

$$\left(M \,\middle|\, \sum_n L_{nz}\left(1 - \frac{z_n^2}{r_n^2}\right) + 4S_{nz}\left(1 - \frac{z_n^2}{r_n^2}\right) \,\middle|\, M\right) = \left(M \,\middle|\, AJ_z + BJ_z^3 \,\middle|\, M\right) \quad (21)$$

are now obtained easily from Eqs. 12 to 20; since they are rather cumbersome expressions, they are not given explicitly here.

$\sum_{if} |S_{if}|^2$ as given by Eq. 12 is readily evaluated with the aid of Eq. 21, and an expression for the scattering cross section that is valid for small angles is obtained.